Cardiovascular Reflections of Sympathovagal Imbalance Precede the Onset of Atrial Fibrillation

Alexander Hammer, Hagen Malberg, Martin Schmidt

Institute of Biomedical Engineering, TU Dresden, Dresden, Germany

Abstract

Sympathovagal imbalance is known to precede the onset of atrial fibrillation (AF) and has been analyzed extensively based on heart rate variability (HRV). However, the relationship between sympathetic and vagal effects before AF onset and their influence on various HRV features have not been fully elucidated. QT interval variability (QTV) reflects sympathetic activity and may therefore provide further insights into this relationship. Using the time delay stability (TDS) method, we investigated temporal changes in coupling behavior before AF onset between 20 vagal or sympathovagal-associated HRV and QTV features. We applied the TDS method to 26 electrocardiograms from the MIT-BIH AF database with at least one hour of sinus rhythm preceding AF onset. Sinus rhythm segments were split into 5-minute windows with 50 % overlap. Logistic regression analysis revealed significantly ($p < 0.01$) increased coupling between QTV and vagal HRV features from 20 to 15 minutes before AF onset. We found similar behavior between QTV and sympathovagal HRV features. This indicates sympathetic predominance increasing until 15 minutes before the onset of AF and decreasing towards vagal predominance right before AF onset. Our results provide new insights into temporal changes of sympathovagal imbalance preceding AF onset and may improve the prediction of AF in clinical applications.

1. Introduction

Atrial fibrillation (AF) is the most common clinically relevant cardiac arrhythmic disease globally and is associated with increased morbidity and mortality [1]. In the beginning, AF usually occurs paroxysmal and becomes persistent over time. There is evidence that the cardiac autonomic nervous system (ANS) is directly involved in the development of AF via an imbalance of the antagonistic vagus nerve and the sympathetic nervous system [2–4]. However, due to the lack of methods for separating sympathovagal effects, the exact interaction remains unclear [3].

Heart rate variability (HRV) reflects cardiac ANS activity, can be easily extracted from the electrocardiogram (ECG), and has been widely used to analyze sympathovagal imbalance before the onset of AF [2]. Features of short-term HRV are strongly related to vagal tone, while others reflect sympathovagal balance [5]. The sympathetic activity can therefore only be inferred indirectly. Recent research suggests that variability in ventricular repolarization, derived from the ECG as QT interval variability (QTV), is a direct measure of sympathetic tone [6]. Therefore, the inclusion of QTV features could advance the understanding of the development of AF.

Previous approaches examined temporal changes before the onset of AF in sympathovagal balance, preferably using frequency-based HRV features [2]. However, the proportions of sympathovagal influence on these features have not been conclusively clarified [5]. Analysis of the coupling behavior between different vagal, sympathetic, and sympathovagal-associated features may provide additional information on the changes in sympathovagal balance at the onset of AF. Using the time delay stability (TDS) method [7], we, therefore, examined the coupling behavior between 20 primarily sympathetic, vagal, or sympathovagal-associated HRV and QTV features to generate new insights into the sympathovagal imbalance before the onset of AF. This may be of advantage in clinical applications for predicting AF.

2. Methods

2.1. Data

We used the first lead (Channel not documented) of ECGs from the MIT-BIH AF database (AFDB) [8,9] showing minimum one hour of normal sinus rhythm (NSR) preceding AF for analyzing temporal changes in the sympathovagal coupling before the AF onset ($n_{AF} = 28$ segments from 19 subjects).

2.2. Preprocessing

All ECGs were band-pass filtered between 0.3 Hz and 120 Hz and notch filtered at 60 Hz, using zero-padding to avoid boundary effects. Subsequently, QRS complexes

were detected [10] and corrected, based on amplitude heights and signs as well as peak-to-peak and peak-to-signal edge distances [11]. We applied iterative two-dimensional signal warping (i2DSW) [12, 13] to robustly extract RR- and QT intervals as well as T wave amplitudes on a beat-to-beat basis [14]. Subsequently, noisy heart beats and abnormal RR intervals were rejected [12].

2.3. Feature Extraction

We extracted 12 HRV and 8 QTV features for windows of 5 minutes length [6, 15] with a stepsize of 5 s. Windows were excluded if more than 50 % of RR and QT intervals have been rejected. We calculated standard HRV and QTV features, including the standard deviation of RR (SDRR) and QT intervals (SDQT) as well as the root mean square (RMSSD) and standard deviation (SDSD) of successive RR differences. Furthermore, we extracted the short- and long-term variability of RR (STVRR, LTVRR) and QT intervals (STVQT, LTVQT) [16], respectively. As additional features for short- versus long-term HRV, we included the Poincaré features SD1, SD2, and SD1SD2ratio. The feature set was supplemented by features quantifying the spectral density of high (HF), low (LF), and very low (VLF) frequencies as well as the ratio of low and high frequencies (LFHFratio) from the interpolated RR tachogram and similarly from QT tachogram ($\mathrm{LF_{QT}}$, $\mathrm{HF_{QT}}$, $\mathrm{LFHFratio_{QT}}$). Finally, we calculated the T wave amplitude corrected SDQT (cSDQT) and QTV (cQTV) to account for the inverse relationship between QTV and T wave amplitude [17]. While HRV features reflecting short-term or high-frequency HRV (RMSSD, SDSD, STVRR, SD1, and HF) are dominated by more rapid vagal activity, the remaining HRV features (SDRR, LTVRR, SD2, SD1SD2ratio, LFHFratio, VLF, LF) reflect both vagal and sympathetic activity [5]. Calculated features can thus be divided into three domains: vagal HRV features ($\mathrm{HRV_V}$), sympathovagal HRV features ($\mathrm{HRV_{S/V}}$), and predominately sympathetic QTV features.

2.4. Coupling Analysis

We used the TDS method [7] to quantify the coupling behavior, which considers two signals to be coupled if the temporal shift of common fluctuations remains stable over several windows. The proportion of stable windows gives information about the coupling strength in %TDS.

All feature time series have been z-normalized. The temporal shift was determined in 5-minute windows with 50 % overlap using cross-correlation and was assumed to be stable for each window i unless deviated by more than 2 in the two windows before and after. To avoid random effects, we applied surrogate tests by calculating the coupling between the signals of each subject with signals from another randomly and uniquely selected subject.

2.5. Statistical Analysis

To analyze temporal changes, we first averaged segments, adjusted by surrogate test, and then calculated the differences between the baseline, defined as the window before the AF onset (preAF), and windows further ahead. Subsequently, we applied logistic regression according to [14] to determine the separability of each window from preAF. Logistic regression was applied to the coupling within and between the 3 feature domains. For each of the analyses, Bonfferoni-Holm correction was applied to account for multiple comparisons to baseline.

All signal processing and statistics were done with Matlab R2021b (MathWorks Inc., Natick, MA, USA).

3. Results of Coupling Analysis

Two ECG segments had to be excluded after removal of noisy heart beats and abnormal RR intervals, leaving $n_{AF} = 26$ segments. We found statistically significant ($p < 0.01$) fluctuations in the coupling between $\mathrm{HRV_{S/V}}$ or $\mathrm{HRV_V}$ and QTV features, respectively (see Table 1), between 22.5 to 15 minutes before AF onset. In both cases, a drop followed by an increase in the coupling strength could be determined from about 30 minutes before AF onset, with the maximum coupling strength of 4.5 ± 5.9 %TDS (QTV–$\mathrm{HRV_{S/V}}$) and 6.9 ± 9.3 %TDS (QTV–$\mathrm{HRV_V}$) being reached 15 minutes before AF onset. The time course of the coupling behavior between QTV and $\mathrm{HRV_V}$ signals is illustrated in detail in Figure 1. Neither between features of the same domain nor between $\mathrm{HRV_{S/V}}$ and $\mathrm{HRV_V}$ features, any significant changes in coupling strength have been observed before the onset of AF. Only a trend in the form of an increase from about 25 minutes before AF onset with a subsequent decrease in the coupling strength, similar to Figure 1, could be determined for couplings of features within the domains of $\mathrm{HRV_{S/V}}$ and QTV. Opposing trends were found for the coupling between $\mathrm{HRV_{S/V}}$ and $\mathrm{HRV_V}$ as well as for the coupling within the $\mathrm{HRV_V}$ domain.

4. Discussion and Conclusion

The significant increase after a previous drop in the coupling between sympathetic related QTV features and $\mathrm{HRV_V}$ features suggests an increasing sympathovagal coupling from about 30 minutes before the onset of AF. The similar course of coupling between $\mathrm{HRV_{S/V}}$ and QTV features indicates a decreasing vagal influence on HRV and sympathetic predominance. This is supported by the opposite trend of coupling between $\mathrm{HRV_{S/V}}$ and $\mathrm{HRV_V}$ features, which suggests decreasing vagal and increasing sympathetic reflections in $\mathrm{HRV_{S/V}}$ features. This indicates an

Table 1. Changes in coupling strength between features of the domains of sympathovagal-associated $HRV_{S/V}$, vagal-associated HRV_V, and sympathetic-associated QTV, compared to baseline, given by mean and standard deviation in %TDS. The baseline was defined as the window directly preceding atrial fibrillation (AF) onset. Furthermore, the number of feature combinations n per domain is given. Significant differences according to logistic regression analysis are indicated as follows: $^*p < .05$, $^{**}p < .01$, $^{***}p < .001$, $^\dagger p < .05$ before Bonfferoni-Holm correction.

Domains	n		**Time to AF onset in minutes**																
			7.5	**10**	**12.5**	**15**	**17.5**	**20**	**22.5**	**25**	**27.5**	**30**	**32.5**	**35**	**37.5**	**40**	**42.5**	**45**	**47.5**	**50**
$HRV_{S/V}$-$HRV_{S/V}$	21	%TDS	1.6 ±5.1	3.1 ±8.6	6.4 ±10.0 †	6.4 ±9.1 †	2.9 ±9.7	−0.5 ±10.3	−2.7 ±7.5	−3.5 ±7.9	−3.3 ±5.5 †	0.2 ±10.4	0.2 ±9.6	−2.4 ±11.0	−2.9 ±11.4	−4.6 ±10.7	−3.5 ±9.0	−1.1 ±10.7	0.7 ±10.8	4.2 ±8.4
$HRV_{S/V}$-HRV_V	35	%TDS	−0.2 ±4.0	1.0 ±6.9	−0.9 ±9.5	−3.2 ±9.5	−4.2 ±12.6	−2.3 ±9.8	−1.2 ±9.4	−0.4 ±8.1	−1.8 ±8.9	4.1 ±8.9 †	0.5 ±12.2	−0.3 ±11.5	2.7 ±12.7	1.3 ±10.8	1.4 ±8.6	5.8 ±9.6 †	3.0 ±8.1	3.7 ±8.0 †
QTV-$HRV_{S/V}$	56	%TDS	0.5 ±3.6	1.3 ±4.9	2.3 ±6.2 †	4.5 ±5.9 ***	4.2 ±6.3 **	4.1 ±8.4 *	2.1 ±7.1 †	1.0 ±7.2	1.0 ±8.4	−1.2 ±7.9	2.1 ±6.5 †	1.9 ±6.9 †	1.7 ±5.3 †	0.8 ±5.7	−0.6 ±6.5	1.9 ±7.6	−0.5 ±8.1	1.8 ±7.6
HRV_V-HRV_V	10	%TDS	0.4 ±1.2	1.5 ±1.9	−3.1 ±2.3	−3.8 ±3.0	−1.2 ±1.8	0.0 ±3.0	1.5 ±1.9	4.6 ±5.7	2.3 ±3.5	1.5 ±1.9	2.7 ±3.5	1.5 ±4.6	−1.2 ±1.8	−1.2 ±1.8	0.4 ±3.2	−1.9 ±7.1	2.3 ±8.1	5.0 ±14.1
QTV-HRV_V	40	%TDS	1.1 ±4.9	1.8 ±4.9 †	5.5 ±10.4 †	6.9 ±9.3 **	5.7 ±6.7 **	6.8 ±7.7 **	4.4 ±5.6 **	1.9 ±5.7 †	2.2 ±7.1	−0.2 ±6.1	0.3 ±8.8	1.8 ±7.8	2.6 ±6.4 †	1.3 ±6.5	1.3 ±7.7	2.8 ±8.7	4.0 ±11.0 †	2.5 ±8.3
QTV-QTV	28	%TDS	1.6 ±5.4	0.7 ±7.3	2.3 ±8.9	2.3 ±8.6	3.8 ±6.1 †	1.2 ±8.5	−0.5 ±6.1	−1.5 ±7.9	0.4 ±7.0	1.2 ±8.4	−0.5 ±7.0	1.5 ±8.1	4.3 ±7.3 †	3.0 ±9.3	4.1 ±6.6 †	3.2 ±8.2	3.0 ±8.7	−1.6 ±6.5

increasing sympathetic predominance until about 15 minutes before the onset of AF, which sharply decreases towards vagal predominance just before the onset of AF, and is consistent with the results from [18].

In [14], we identified changes in P wave and PQ interval morphology about 10 minutes before AF onset as a predictor of AF onset, based on the same database. We hypothesized that preliminary, self-terminating fibrillatory waves superimpose on the ECG signal, causing a change in morphology. According to [4], the sympathetic and vagus nerves affect the electrophysiological properties of sinus nodes and atria differently. While sympathetic activity increases the action potential frequency in sinus node and atria, vagus nerve stimulation leads to an irregular shortening of the action potential duration and to the occurrence of delays in transmission, which complementary promotes re-entry mechanisms. Based on our new results, it can be concluded that a shift towards sympathetic predominance up to 15 minutes before the onset of AF leads to vagal hyperactivation and the occurrence of the first re-entry cycles. The combination of a sympathetically increased action potential frequency and a vagally reduced action potential duration then leads to AF onset [2].

It is at least debatable whether QTV features are a marker of sympathetic activity. Evidence for the correlation between QTV and sympathetic activity was primarily found in healthy people and people with pathologically increased sympathetic tone [6]. Therefore, we applied our methods to the MIT-BIH NSR database [**?**] and compared the time-averaged coupling between the features of the different domains of healthy subjects (NSRDB) and subjects with AF (AFDB) using Student's *t*-test. As presented in Table 2, no significant differences were found.

To best of our knowledge, we were the first to apply the TDS method to HRV and QTV features and, moreover, to investigate the coupling between QTV and $HRV_{S/V}$ or HRV_V. Our results confirm the current state of the literature and provide new insights into the onset of sympathovagal imbalance prior to AF onset based on ECG features that are either related to sympathetic or vagal activity or both. Furthermore, we did not find any significant changes in the coupling between features from the same domain, suggesting that the features reflect roughly the same effects. However, there are trends (e.g. within the

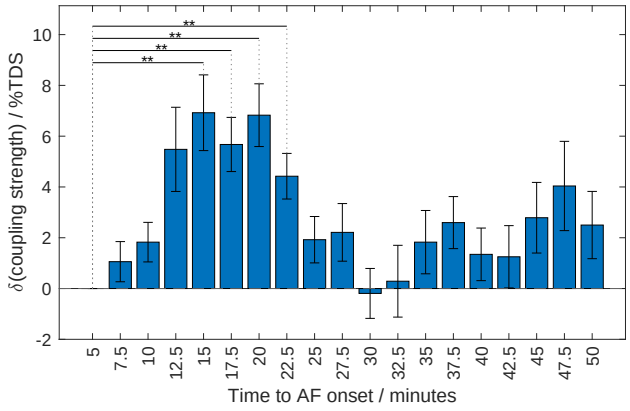

Figure 1. Mean differences $\delta \pm$ standard error in coupling strength between primarily sympathico related QTV features and vagal HRV features (HRV_V) compared to baseline. The baseline was defined as the windows, ending 5 minutes before the onset of atrial fibrillation (AF). Significant differences according to logistic regression after correction for multiple testing were indicated (**: $p < .01$).

Table 2. Results of Student's *t*-test on differences in coupling strength (mean ± standard deviation) in sympathovagal associated $HRV_{S/V}$ features, vagal associated HRV_V features, and QTV features between subjects with AF [8,9] and healthy subjects [9].

	%TDS		t	p
	AF	**healthy**		
$HRV_{S/V}$	12.6 ± 18.8	14.0 ± 20.6	-0.6	0.6
HRV_V	18.0 ± 27.5	15.7 ± 28.8	0.6	0.6
QTV	13.7 ± 25.6	13.1 ± 24.2	0.2	0.8

$HRV_{S/V}$ domain) that are similar to the course of the coupling change between $HRV_{S/V}$ and HRV_V and could become significant with larger sample size.

To conclude, we have for the first time investigated the well known sympathovagal imbalance before the onset of AF by analyzing the coupling of a variety of ECG features. In addition to commonly used HRV features, we used sympathetic predominated QTV features. Our results reveal a significant reversal in sympathovagal balance toward sympathetic predominance that begins 30 minutes before onset of AF, peaks 15 minutes before onset, and swings toward parasympathetic predominance. These new findings about the temporal progress of sympathovagal imbalance preceding the onset of AF may extend previous knowledge on the onset of AF and help predict AF in clinical applications.

Acknowledgments

This study was supported by grants from the European Union's Horizon 2020 research and innovation program (TIMELY, No. 101017424).

References

[1] Chugh SS, Havmoeller R, Narayanan K, Singh D, Rienstra M, Benjamin EJ, Gillum RF, Kim YH, McAnulty JH, Zheng ZJ, Forouzanfar MH, Naghavi M, Mensah GA, Ezzati M, Murray CJ. Worldwide Epidemiology of Atrial Fibrillation. Circulation 2014;129(8):837–847.

[2] Khan AA, Lip GYH, Shantsila A. Heart rate variability in atrial fibrillation: The balance between sympathetic and parasympathetic nervous system. Eur J Clin Invest 2019; 49(11):e13174.

[3] Qin M, Zeng C, Liu X. The cardiac autonomic nervous system: A target for modulation of atrial fibrillation. Clin Cardiol 2019;42(6):644–652.

[4] Coumel P. Paroxysmal atrial fibrillation: A disorder of autonomic tone? Eur Heart J 1994;15 Suppl A:9–16.

[5] Shaffer F, Ginsberg JP. An Overview of Heart Rate Variability Metrics and Norms. Front Public Health 2017;5:258.

[6] Baumert M, Porta A, Vos MA, Malik M, Couderc JP, Laguna P, Piccirillo G, Smith GL, Tereshchenko LG, Volders PGA. QT interval variability in body surface ECG: Measurement, physiological basis, and clinical value: Position statement and consensus guidance endorsed by the European Heart Rhythm Association jointly with the ESC Working Group on Cardiac Cellular Electrophysiology. Europace 2016;18(6):925–944.

[7] Bashan A, Bartsch RP, Kantelhardt JW, Havlin S, Ivanov PC. Network physiology reveals relations between network topology and physiological function. Nat Commun 2012; 3(1):702.

[8] Moody GB, Mark RG. A New Method for Detecting Atrial Fibrillation Using R-R Intervals. Comput Cardiol 1983; 10:227–230.

[9] Goldberger A, Amaral L, Glass L, Hausdorff J, Ivanov PC, Mark R, Mietus JE, Moody GB, Peng CK, Stanley HE. PhysioBank, PhysioToolkit, and PhysioNet: Components of a New Research Resource for Complex Physiologic Signals. Circulation Online 2000;101(23):e215–e220.

[10] Johnson AE, Behar J, Andreotti F, Clifford GD, Oster J. R-Peak Estimation Using Multimodal Lead Switching. In Comput. Cardiol. September 2014; 281–284.

[11] Hammer A, Scherpf M, Ernst H, Weiß J, Schwensow D, Schmidt M. Automatic Classification of Full- And Reduced-Lead Electrocardiograms Using Morphological Feature Extraction. In Comput. Cardiol., volume 48. Brno, Czech Republic, September 2021; 1–4.

[12] Schmidt M, Baumert M, Porta A, Malberg H, Zaunseder S. Two-Dimensional Warping for One-Dimensional Signals—Conceptual Framework and Application to ECG Processing. IEEE Trans Signal Process 2014;62(21):5577–5588.

[13] Schmidt M, Baumert M, Malberg H, Zaunseder S. Iterative two-dimensional signal warping—Towards a generalized approach for adaption of one-dimensional signals. Biomed Signal Process Control 2018;43:311–319.

[14] Hammer A, Malberg H, Schmidt M. Towards the Prediction of Atrial Fibrillation Using Interpretable ECG Features. In Comput. Cardiol., volume 49. Tampere, Finland, September 2022; 1–4.

[15] Task Force of the European Society of Cardiology the North American Society of Pacing Electrophysiology. Heart Rate Variability. Circulation 1996;93(5):1043–1065.

[16] Berger RD, Kasper EK, Baughman KL, Marban E, Calkins H, Tomaselli GF. Beat-to-Beat QT Interval Variability: Novel Evidence for Repolarization Lability in Ischemic and Nonischemic Dilated Cardiomyopathy. Circulation 1997; 96(5):1557–1565.

[17] Schmidt M, Baumert M, Malberg H, Zaunseder S. T Wave Amplitude Correction of QT Interval Variability for Improved Repolarization Lability Measurement. Front Physiol 2016;7:216.

[18] Bettoni M, Zimmermann M. Autonomic Tone Variations Before the Onset of Paroxysmal Atrial Fibrillation. Circulation 2002;105(23):2753–2759.

Address for correspondence:

Alexander Hammer
Institute of Biomedical Engineering, TU Dresden
Fetscherstr. 29, 01307 Dresden, Germany
alexander.hammer@tu-dresden.de